Proc. NIPR Symp. Polar Meteorol. Glaciol., **8**, 66–80, 1994

MICROMETEOROLOGICAL OBSERVATION OVER THE FAST ICE AT ONGUL STRAIT NEAR SYOWA STATION

Kiyotaka NAKAGAWA

Division of Science, Joetsu University of Education, Yamayashiki-machi, Joetsu 943

Abstract: Micrometeorological conditions were observed over fast ice with overlying thick snow cover and underlying deep sea approximately in the center of Ongul Strait in Lützow-Holm Bay, Antarctica, from the end of March to the beginning of December in 1990. In response to the annual change of solar radiation, the radiation balance had an annual change; the radiation balance was negative for a period including the polar night, and changed to positive after October. Corresponding to the radiation balance, both the sensible heat flux from the air to the snow and the conductive heat flux from the fast ice to the snow changed. Especially, the sensible heat flux changed with the radiation balance like a mirror image. As the prevailing wind velocity increased, the temperature and humidity increased, and the radiative heat loss, the sensible heat flux from the air to the snow, and the conductive heat flow from the fast ice to the snow decreased.

1. Introduction

The appearance of sea ice seems to influence strongly the sea-atmosphere interaction in Lützow-Holm Bay. In spite of the importance of the sea ice, few studies have observed directly the micrometeorological conditions over the sea ice with underlying deep sea in this area. Although a few studies have observed the micrometeorological conditions over the sea ice (*e.g.* MAKI, 1974; ISHIKAWA *et al.*, 1982), since they were done near and/or leeward of Syowa Station, which is built on a rocky area without snow or ice, they had several problems: insufficient fetch for the prevailing wind, insufficient sea depth, insufficient observation duration, contamination of the snow and ice surface, and so on. In addition, recently the importance of such observations as ground truth data for satellite remote sensing has been increasing. However, since the resolution of the NOAA/AVHRR data is 1.1 km at the subpoint of the satellite, the observation sites were included in the same pixel including rock area or Syowa Station Area. Therefore, it is also difficult to utilize the results of the above observations as ground truth data.

The purpose of the present study is to observe micrometeorological conditions at a fixed site over the fast ice that can represent a wide region near Lützow-Holm Bay. Of course, such observations must be done at a site on the fast ice both with sufficient fetch for northeasterly wind and with sea depth of hundreds of meters significantly off Syowa Station for as long a duration as possible.

2. Site Description

Figure 1 is a general view of the study area. East Ongul Island, where Syowa Station is located, is about 4–5 km westward off the Sôya Coast of the Antarctic continent. Between the Antarctic continent and East Ongul Island, there is Ongul Strait with maximum sea depth of more than 600 m. The Antarctic continent is covered with a thick ice sheet, the altitude of the continent being approximately equal to the thickness of the ice sheet. On the other hand, East Ongul Island is almost snow free even in winter. The strait had been covered with stable fast ice continuously for more than 3 years. Although the eastern part of the fast ice of Ongul Strait was bare, the western part was covered with snow. The depth of the snow cover increased westward from the middle of the strait.

The solid circle is the observation site, about 2 km eastward off the station. The sea depth at the site was 330 m, and we always had more than 120 cm thick fast ice during the whole year. Since the prevailing wind direction was northeast,

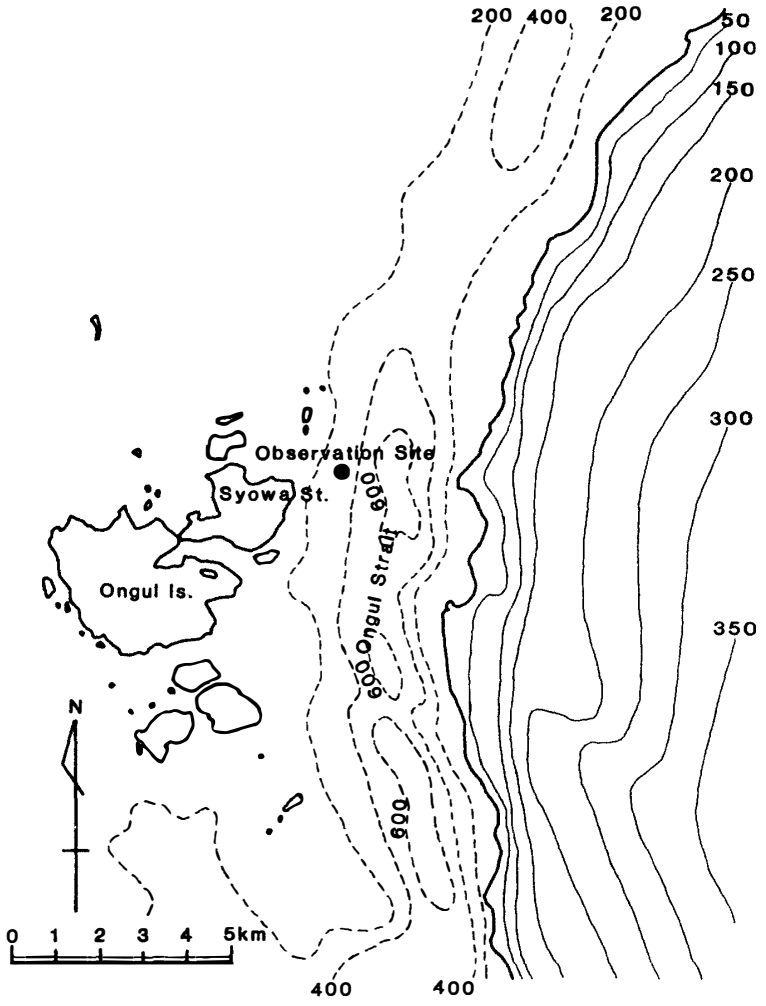

Fig. 1. Map of the study area. Solid circle: the micrometeorological observation site. Solid lines: the contour lines every 50 m; dashed lines: isolines of sea depth every 200 m.

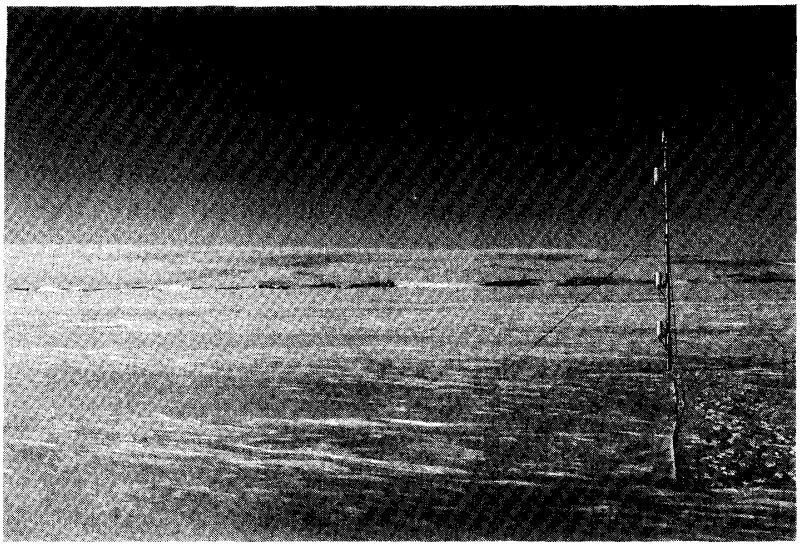

Fig. 2. Instrumentation for the wind, air temperature and relative humidity on the pole (April 2, 1990).

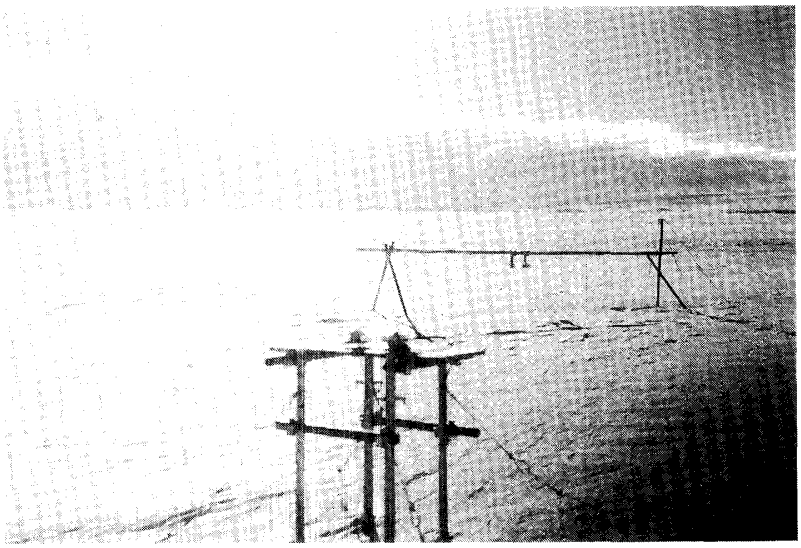

Fig. 3. Instrumentation for radiation (April 2, 1990).

the fetch for the wind of this site was large enough to observe standard micrometeorological conditions over the fast ice.

An aluminum pole with height of 5 m was set on the fast ice surface, and supported by 3 stays. Figure 2 shows the instrumentation on the pole. At 3 levels, 1, 2 and 4 m above the fast ice surface, horizontal arms were attached to hold instruments for measuring wind velocity, air temperature and relative humidity. Wind direction was observed at the top of the pole.

Platforms for radiation instruments shown in Fig. 3 were constructed 40 m northward of the pole. The downward shortwave, downward longwave, upward shortwave and upward longwave radiations were measured separately by different instruments.

Three thermistor thermometers were set in the snow and ice near the pole. One was on the interface between the fast ice and the snow cover, another was in the fast ice at 5 cm depth, and the other was left alone in the snow cover over the fast ice.

All the variables were measured every 10 min, and outputs from sensors were digitized and stored by the data loggers. The accumulated values of wind velocity and radiation fluxes, and instantaneous vales of other variables, were recorded. The data loggers were changed every few months, and the stored data were transferred to a computer and floppy disks at Syowa Station.

3. Results and Discussion

After all the preparations were finished, the system began to operate at 0000 LST on March 27, 1990, in the middle of very severe drifting snow, a so-called blizzard. After that, the long term observations until December 9, 1990 succeeded in spite of some troubles, such as lack of power supply to loggers and humidity sensors, disconnection of communication cables, burying of meteorological sensors in the snow, and so on. The observations stopped on the morning of December 10, 1990 when sea water updrifted through fast ice of thickness more than 150 cm and most parts of the loggers and transmitters were destroyed by salt water. Thus, continuous micrometeorological data over the fast ice were obtained for a period of more than 8 months including the polar night.

Figure 4 shows the seasonal change of snow cover depth at the observation site. Although the snow cover depth was measured with a standard snow gauge network about 100 m westward of the site, the spatial variation was very large. So the present study shows the snow depth measured at the site using a pole in the place of the snow gauge. For about 2 months from the beginning of the observation, the snow cover depth remained almost constant, *i.e.* about 10 cm.

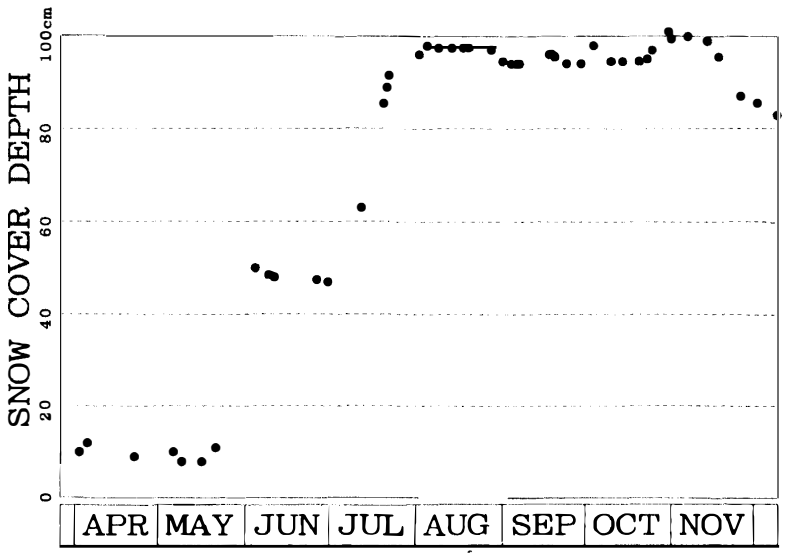

Fig. 4. Annual variations of snow cover depth at the observation site.

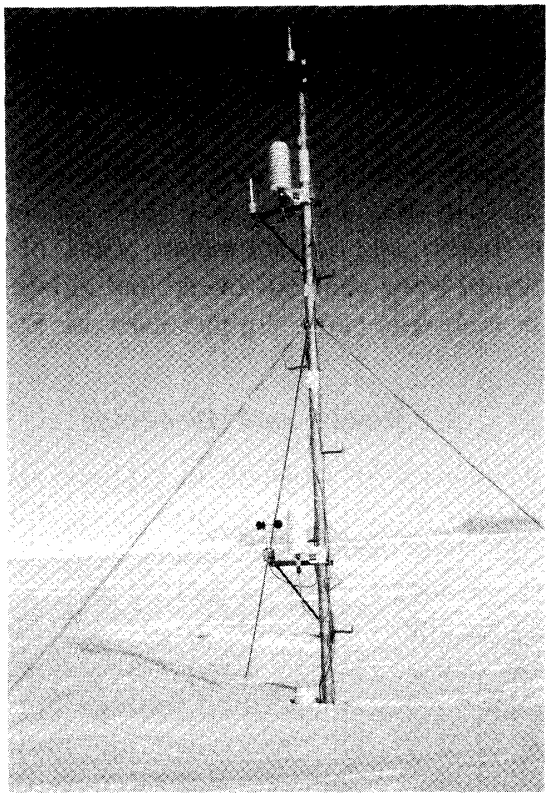

Fig. 5. The observation pole after heavy snow fall (November 1, 1990).

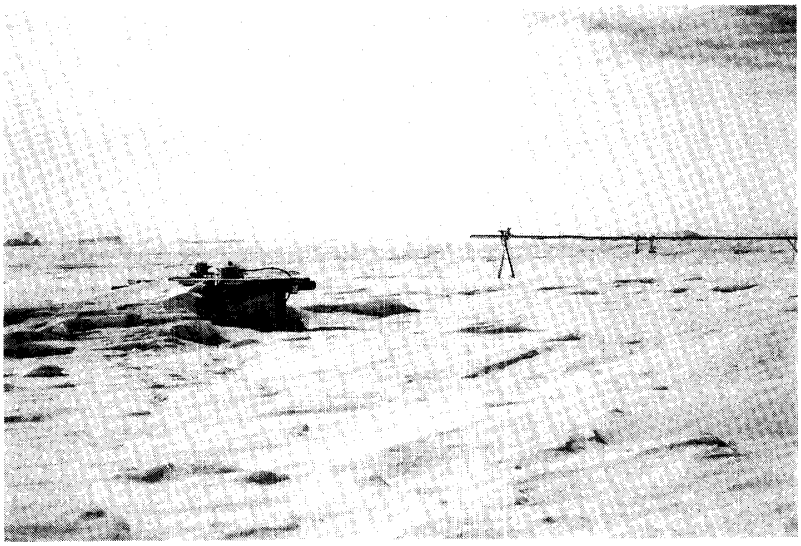

Fig. 6. Radiation instruments after heavy snow fall (November 1, 1990).

Although strong snow drifts occurred often in April and May, the snow cover depth did not change. However, after the severe snow drift at the beginning of June, the snow cover depth increased to about 50 cm, and then remained almost constant again for about 1 month. We had several blizzards in July, and could

not leave Syowa Station. The snow cover depth rapidly increased at every measurement, reaching 1 m at the begging of August. Although there were repeated small increases and decreases, the snow cover depth remained almost constant until the middle of November. The maximum snow cover depth of 101 cm occurred on October 30, 1990. Figures 5 and 6 show the observation site on November 1, 1990. All the sensors for wind velocity, air temperature and relative humidity at the height of 1 m above the fast ice surface were completely buried in the snow cover. After that, the snow cover depth started gradually decreasing, reaching 80 cm at the beginning of December.

Figure 7 shows the day-to-day variations of the components of solar radiation. The heavy solid line stands for the daily total solar radiation flux at the top of the atmosphere, which was calculated astronomically from the latitude of Syowa Station and the orbital parameters of the sun. The solar radiation at the top of the atmosphere at the begging of the observation was already not so strong, *i.e.* about 10 MJ/m^2·d, and decreased rapidly. The solar radiation vanished at this site from the end of May through the middle of July. After the polar night, the daily total solar radiation rapidly increased, exceeding 40 MJ/m^2·d at the middle of November.

The total column gives the daily total of global solar radiation, and the solid column the daily total of reflected solar radiation. They are shown only for days without missing data, *i.e.* 144 observations. The daily total solar radiation was, of course, large on the fine weather day, and small on an overcast day. Therefore, although the global solar radiation had a clear annual cycle parallel to the solar

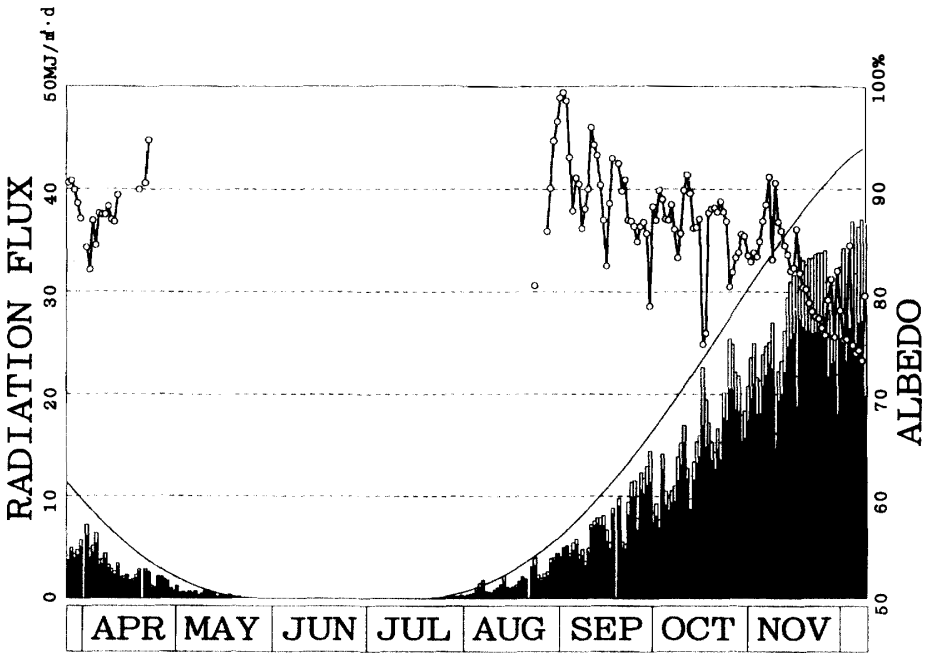

Fig. 7. Annual variations of solar radiation. Solid line: calculated global solar radiation at the top of the atmosphere. Total columns: observed global solar radiation; solid columns: observed reflected solar radiation. Open circles with zigzag line: the calculated surface albedo.

radiation at the top of the atmosphere, there were also day-to-day variations due to weather conditions. The daily global solar radiation was largest in early summer, reaching 35 MJ/m^2·d when the weather was good. This was probably due both to the high transmissivity of the atmosphere and to the high albedo of the underlying snow surface (TAKEUCHI and KONDO, 1981).

Naturally, the variations of the reflected solar radiation corresponded well to those of the global solar radiation. From the beginning of the observations through September, there was little difference between global and reflected solar radiations; most of the global radiation was reflected upward. After that, the difference between both radiations increased gradually.

The open circles linked with the solid line represent the variations of surface albedo, defined as the ratio of upward reflected solar radiation flux to the downward solar radiation flux at the surface. They are plotted only for days with global solar radiation larger than 2.5 MJ/m^2·d. Although the surface albedo did not show a clear annual cycle as did the solar radiation, a weak annual cycle of the surface albedo of the snow cover over the fast ice was seen; it was higher in spring than in early summer, probably due to changes in the snow density, liquid water content, and solar elevation (WARREN, 1982). Although the surface albedo exceeded 95% at the beginning of September, after that it decreased gradually, and it reaching 70% in December. There were also day-to-day variations in the surface albedo corresponding to variations of the global solar radiation.

Figure 8 shows day-to-day variations of components of the radiation balance at the surface. The solid zigzag line is the daily total global solar radiation flux shown by the total columns in Fig. 7. The upward total columns are the solar radiation absorbed by the surface. These data are shown only for days when all the components of radiation are available. Since the surface albedo was very high, although the global solar radiation flux was very large, the solar radiation absorbed by the surface was small, almost negligible from the beginning of April through the middle of September. After that, the absorbed solar radiation increased gradually, reaching 10 MJ/m^2·d at the beginning of December.

The downward total columns are the effective longwave radiation. The downward longwave radiation flux increased under overcast conditions, which resulted in decrease of effective longwave radiation. As a result, the longwave radiation balance included large day-to-day variations, whereas there did not exist a clear annual cycle. In the case of a cloudless sky, the energy loss due to the negative longwave radiation balance exceeded 5 MJ/m^2·d.

Solid columns are the daily total radiation balance at the surface, *i.e.* the difference between the absorbed solar radiation and the effective longwave radiation. It is clear that negative radiation balance continued from the beginning of the observations through the middle of October. In October the sign of the radiation balance changed day by day, because the magnitudes of the absorbed solar radiation and the effective longwave radiation were comparable. After the end of November, days with positive radiation balance continued. The sign change of the radiation balance of snow over sea ice near Syowa Station in October was also reported by ISHIKAWA *et al.* (1982).

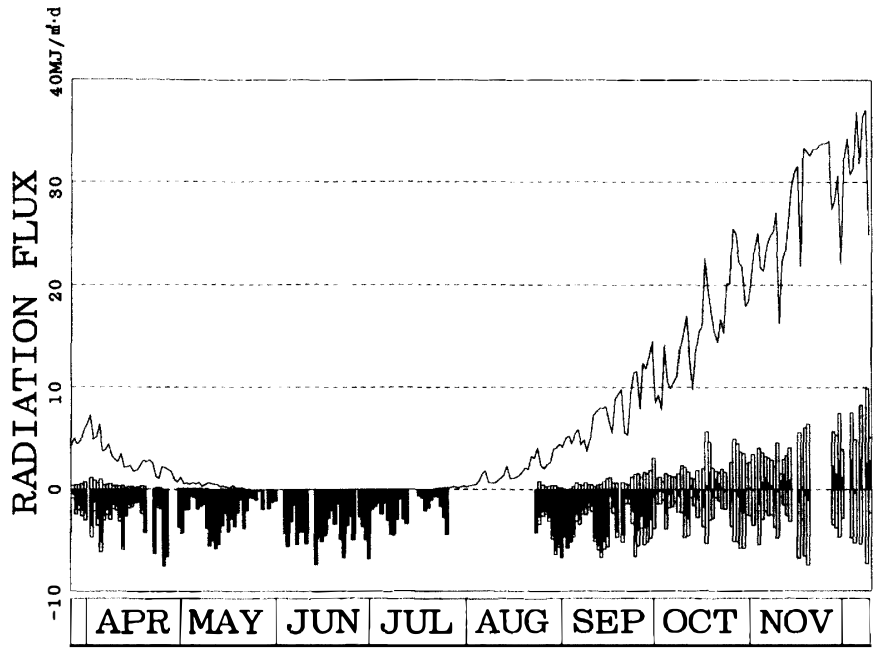

Fig. 8. Annual variations of components of the radiation balance. Zigzag solid line: the observed global solar radiation. Upward total columns: solar radiation absorbed by the snow surface; downward total columns: effective longwave radiation; solid columns: the radiation balance.

Comparing these characteristics of the radiation balance at the surface of the snow cover over the fast ice mentioned above with those over the continental ice sheet, Mizuho Plateau, at an altitude of more than 2000 m (YAMANOUCHI *et al.*, 1981), they are essentially similar to each other, but the magnitude of the radiation balance is slightly larger on oceanic fast ice than on the continental ice sheet. This seems to result from the difference of the surface temperatures due both to the different altitude and to the different underlying heat source.

Figure 9 shows day-to-day variations of wind velocity, air temperature and relative humidity 4 m above the fast ice surface. The open columns at the bottom are daily mean wind velocities. The prevailing wind was northeasterly, especially during strong wind. Whenever a low pressure system approached the study area, a strong northeasterly wind blew. In addition, the katabatic wind, also northeasterly, blew often in winter. The katabatic wind usually started blowing at midnight and stopped at noon, and was not strong. Large daily mean wind velocity exceeding 10 m/s was introduced by the approach of the low pressure systems. In July we had several blizzards.

The zigzag solid line stands for the daily mean air temperature. A gradual decrease of air temperature was superimposed on the day-to-day scatter since the beginning of the observations. The coldest season was at the end of August. After that the air temperature increased gradually, with day-to-day scatter. After the middle of November the air temperature remained relatively high and the day-to-day scatter decreased. It is clear that the day-to-day scatter of the air temperature corresponded to change of the prevailing wind velocity; the stronger

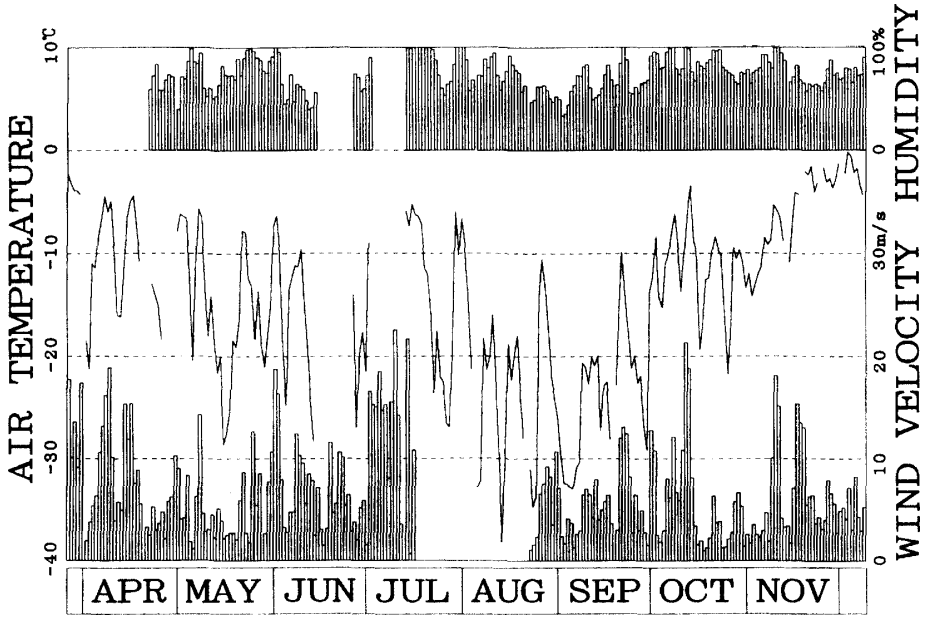

Fig. 9. Annual variations of air temperature (the solid line), the relative humidity (upper open columns) and wind velocity (lower open columns) at 4 m above the fast ice surface, respectively.

the northeasterly wind, the higher the air temperature. Even in midwinter, when the strong northeasterly wind blew, the air temperature rapidly increased above −10°C. This is considered to the result from not only destruction of the surface inversion layer but also advection of warm air from the northern ocean area. On the other hand, when a gentle southerly wind blew, the air temperature was low. This is considered to the result from not only strong radiative cooling but also advection of cold air by the gentle southerly wind.

The open columns at the top are relative humidities. From the beginning of the observation period through the end of April the humidity sensor outputs were not usable because of the lack of electric current from the power supply. After the change of power supply from regulators to an external air battery, the outputs of the humidity sensors seemed to be usable. The relative humidity also changed day by day corresponding to the change of wind velocity; the stronger the northeasterly wind, the higher not only the air temperature but also the relative humidity. This is considered to the result from the advection of moist and warm air from the northern ocean area.

Figure 10 shows day-to-day variations of wind velocity, air temperature and relative humidity 2 m above the fast ice surface. The characteristics of Fig. 10 are the same as Fig. 9. Of course, the daily wind velocity 2 m above the fast ice surface was slightly weaker than at 4 m. The daily air temperature was slightly lower at 2 m than at 4 m, especially on cold days, which suggests that sensible heat has a tendency to be transferred from the air to the snow surface through the observation period. The output of the relative humidity sensor had been unusable since the beginning of August.

Figure 11 shows day-to-day variations of the wind velocity, air temperature

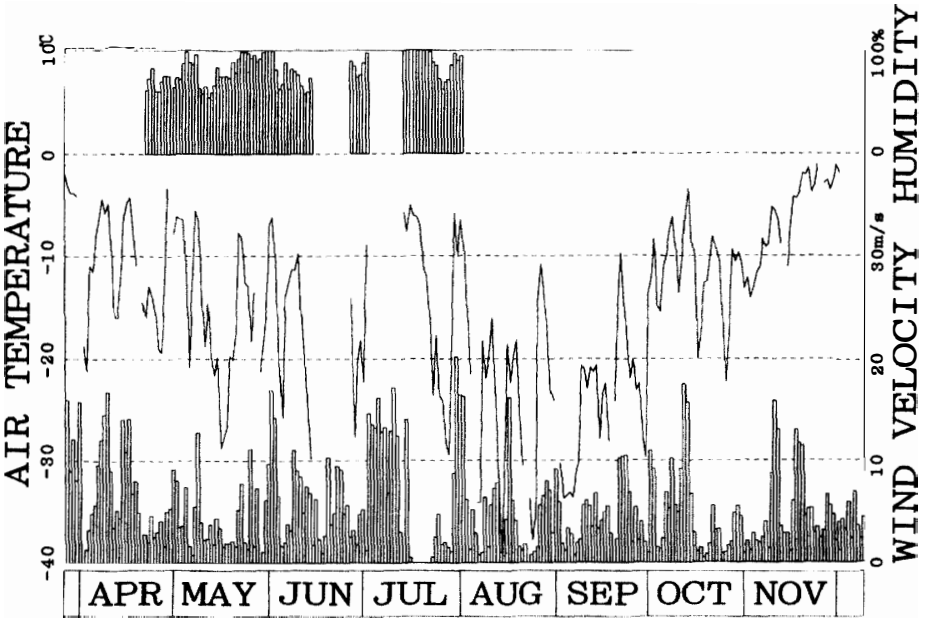

Fig. 10. The same as Fig. 9, but for 2 m above the fast ice surface.

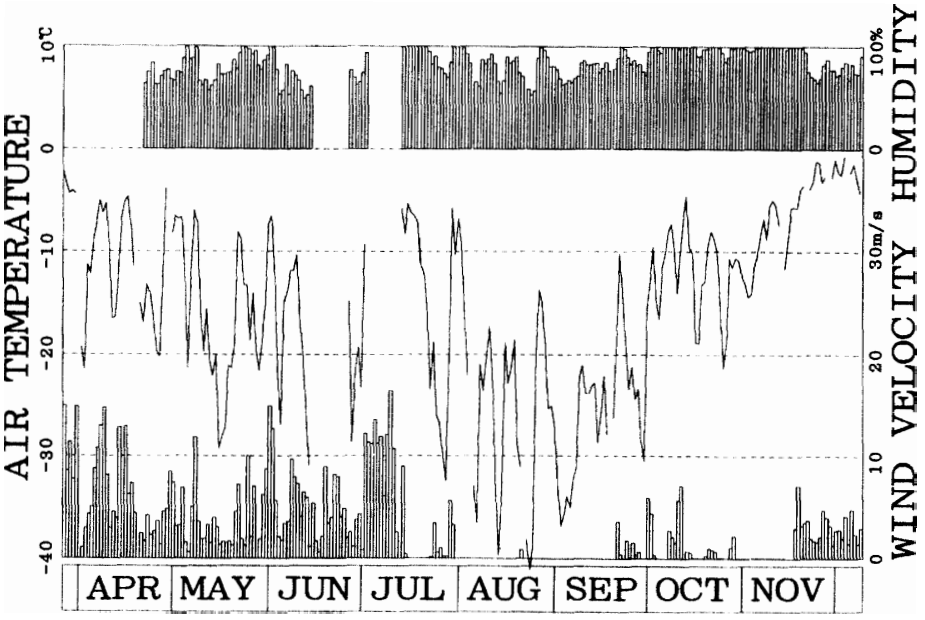

Fig. 11. The same as Fig. 9, but for 1 m above the fast ice surface.

and relative humidity 1 m above the fast ice surface. The characteristics of Fig. 11 are similar to those of Figs. 9 and 10. The wind velocity was weaker and air temperature lower 1 m above the fast ice surface than 4 and 2 m above. The day-to-day change of the relative humidity also corresponded well to those at the other heights. However, it was slightly moister 1 m above the fast ice surface than 4 and 2 m above, being almost saturated from the end of September through the middle of November. This is considered to be because the height of the snow cover surface over fast ice increased to 1 m at the beginning of August.

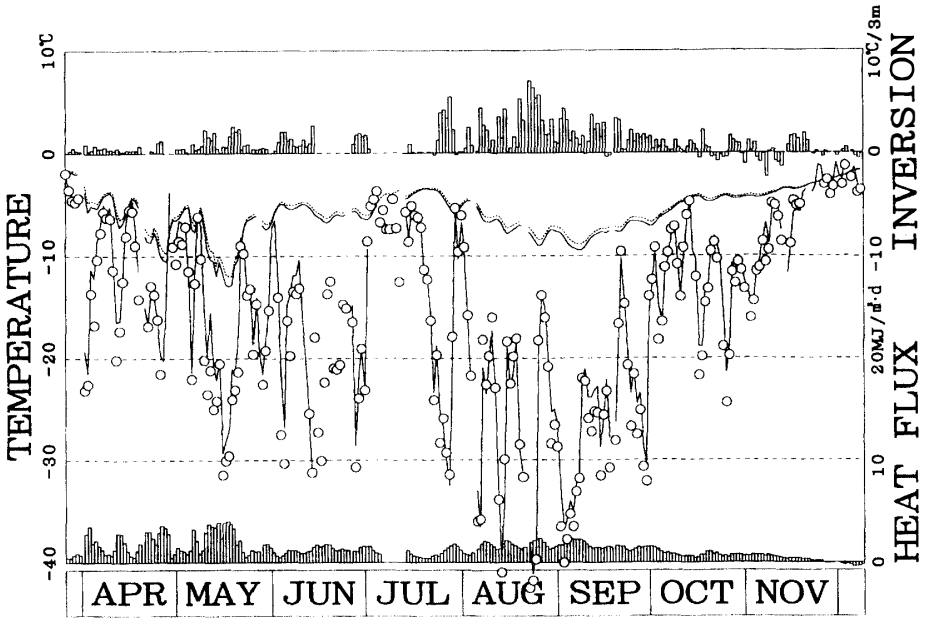

Fig. 12. Annual variations of ice temperatures at 0 and 5 cm depths (smooth solid and dotted lines, respectively), the conductive heat flux from the fast ice to the snow cover (lower open columns), surface inversion intensity (upper open columns), air temperature at 1 m height (zigzag solid lines), and calculated snow surface temperature (open circles).

Since the instruments at 1 m above the fast ice were frequently buried in the snow, the anemometer frequently stopped, and the temperature and humidity became equal to those at the top of the snow cover layer.

Figure 12 shows day-to-day variations of the snow and ice temperature and the conductive heat flux at the upper part of the fast ice. The solid and dotted zigzag lines with a small amount of day-to-day scatter are ice temperatures at 0 and 5 cm respectively. Although both show complex annual cycles with 2 minima before and after the polar night, the temperature at 5 cm was higher than at the fast ice surface. From the end of May through the beginning of August, including the polar night, the ice temperature was high, probably because of the rapid increase in snow depth and persistence of bad weather days.

The open columns at the bottom are conductive heat flux at the surface of the fast ice, estimated from the temperature difference between 0 and 5 cm, the upward heat flow is expressed as positive. Although the thermal conductivity of sea ice is a function of salinity and temperature, it is not so sensitive to either salinity or temperature in the region less than −4°C (see Fig. 3 of ONO, 1968). The salinities at the top of the fast ice near the observation site were 5.5‰, 7.5‰ and 6.0‰, respectively, on August 3, September 30 and November 20 in 1990 (USHIO, 1994, private communication).

It is clear from Fig. 12 that the temperature of the fast ice surface was usually between −5 and −10°C. So the present study used the constant value of 2.24 W/m·K as the thermal conductivity of the fast ice, which was calculated by eq. (29) of ONO (1968) for sea ice of temperature −7.5°C and salinity 6‰. This

value is equal to the thermal conductivity of pure ice at 0°C.

The temporal change of the conductive heat flux is the inverse of that of ice temperature; the lower the ice temperature became, the larger the upward heat flux became. This means that the temperature gradient at the top of the fast ice varies corresponding to its surface temperature. Although from the beginning of the observation through the middle of May the magnitude of the heat flux was about the same as the radiative heat loss at the snow surface, as shown in Fig. 8, during midwinter the magnitude decreased to about half of the radiative heat loss. After the polar night the magnitude increased slightly to about the same as the radiative heat loss. At the end of November the conductive heat flux at the fast ice surface vanished: after that the direction of the heat flux was reversed. This change of sign of the conductive heat flux in November was also reported by ISHIKAWA *et al.* (1982).

Open circles are snow surface temperatures. These were estimated from upward longwave radiation flux observed at the site, assuming the surface to be a black body. The zigzag line with large day-to-day scatter is air temperature 1 m above the fast ice surface. It is clear that day-to-day variations of the estimated surface snow temperature agreed well with the observed air temperature 1 m above the fast ice surface, especially after August when the snow cover surface remained at about the level of the thermometer, 1 m above the fast ice surface. The good agreement after August suggests that the temperature inferred from the observed upward longwave radiation flux is a good approximation of the surface temperature. There was large day-to-day scatter compared with the ice temperature; sometimes the snow surface temperature became high and comparable to the ice temperature, sometimes the snow surface fell to extremely low temperature, as low as −40°C.

The snow surface temperature changed rapidly corresponding to the change of the wind system. When the wind velocity became strong, as in a blizzard, the snow surface temperature increased sharply and became about the same as the fast ice surface temperature and/or the air temperature. On the other hand, when the wind velocity was very small, the snow surface temperature decreased sharply and became lower than both the fast ice temperature and the air temperature.

The open columns at the top are intensity of the temperature inversion between 1 and 4 m above the fast ice surface. Note that the air temperature sensor heights varied corresponding to growth of the snow cover. The strong inversion occurred frequently before and after the polar night; the maximum inversion occurred at the end of August, exceeding 7°C/3m. This suggests that sensible heat was transferred from the air to the snow surface through almost the whole observation period.

The daily total sensible heat flux from the air to the snow surface, H_0, was estimated using the so-called bulk transfer method (ARYA, 1988) as follows:

$$H_0 = -\frac{\rho c_p k^2 U(\theta-\theta_0)}{\{\ln(\frac{z}{z_0})-\psi_m(\frac{z}{L})\}\{(\ln\frac{z}{z_0})-\Psi_h(\frac{z}{L})\}},$$

where ρ is the air density, c_p is the specific heat of air at constant pressure, k is the von Karman constant, U and θ are the mean wind velocity and potential temperature at measurement height z, θ_0 is the potential temperature at the snow surface, z_0 is the roughness height, L is the Monin-Obukhov length, and ψ_m and ψ_h are Monin-Obukhov similarity functions for normalized, respectively, wind velocity and potential temperature. The present study used air temperature and wind velocity at 4 m above the fast ice, and surface temperature estimated from the upward longeave radiation flux, assuming that the measurement height was constant, *i.e.* 4 m, throughout the observation period, in spite of varying snow surface height. The Monin-Obukhov stability parameter, z/L, was determined from the bulk Richardson number. The roughness height was assumed to be constant, 0.0001 m, which is a typical value of the roughness parameter for snow-covered flat or rolling ground (ARYA, 1988). The annual variations of the resulting estimated sensible heat flux are shown in Fig. 13.

The open columns in the middle of Fig. 13 are sensible heat flux transferred from the air to the snow surface. Since 3 elements, *i.e.* the wind velocity and air temperature at 4 m height and the snow surface temperature, affect this quantity, missing data durations occurred frequently, especially in winter and early spring. However, the characteristics of the annual cycle can be recognized easily. Positive sensible heat flux had continued from the beginning of the observation period through the middle of October. After October the sensible heat flux from the air to the snow surface became small, and sometimes the direction of the heat flow changed.

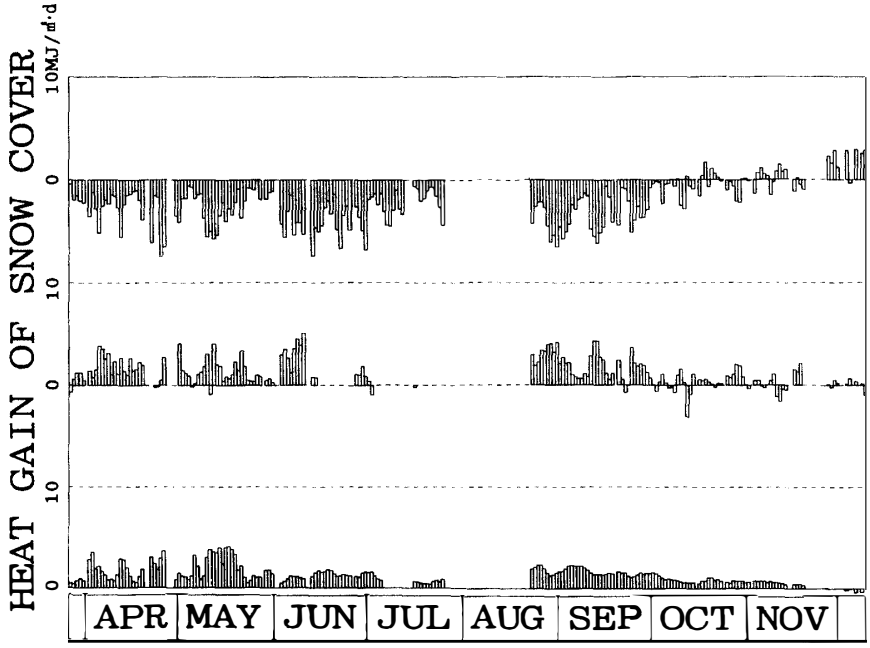

Fig. 13. Comparison of annual variations of components of heat gain of the snow cover. Top: radiation balance; middle: sensible heat flux from the air to the snow cover; bottom: conductive heat flux from the fast ice to the snow cover.

For reference, the annual variations of radiation balance and conductive heat flux from the fast ice to the snow cover are also shown at, respectively, the top and bottom of Fig. 13. It is clear that the radiation balance and the sensible heat flux varied like mirror images, but that the magnitude of the sensible heat flux was slightly smaller than that of the radiation balance. These facts suggest the following: First, the snow surface lost energy due to negative radiation, so that, second, the energy was transferred from the overlying air and the underlying fast ice in order to compensate for the heat loss from the snow surface. However, since the magnitude of the sensible heat flux was not enough, and the conductive heat from the fast ice was blocked by thick snow cover, the snow temperature decreased over time. Since the water vapor content was low because of low temperature, the latent heat gain of the snow surface due to condensation was negligible. After October, the radiation balance became small and at the end of the observation it changed sign.

4. Concluding Remarks

Micrometeorological conditions were observed over fast ice with overlying thick snow cover and underlying deep sea from the end of March to the beginning of December 1990. This was the first micrometeorological observation over sea ice near Syowa Station from before to after the polar night, chiefly because of the stability of the fast ice during that year.

As a result, it is clear that, because of the large annual variation of solar radiation, the radiation balance also varied considerably; the radiation balance was negative for a long period including the polar night, and changed to positive after October. Corresponding to the radiation balance, both the sensible heat flux from the air to the snow and the conductive heat flux from the fast ice to the snow changed. The sensible heat flux varied with the radiation balance like a mirror image.

All of the observed quantities showed day-to-day variations, and varied with the wind velocity; as the prevailing wind velocity increased, the temperature and humidity increased, and the radiative heat loss, the sensible heat flux from the air to the snow, and the conductive heat flux from the fast ice to the snow decreased.

The present study primarily described daily totals or means of observed items. The author plans to analyze diurnal changes and to use the data as ground truth data for satellite remote sensing in the near future.

Acknowledgments

The author wishes to express his sincere thanks to the members of the wintering party of the 31st Japanese Antarctic Research Expedition for their kind assistance in observing the micrometeorological conditions over the fast ice. He is also grateful to Dr. S. Ushio, National Institute of Polar Research, for his useful discussion and comments, and to two anonymous referees for their comments

which were useful in revising this paper.

References

ARYA, S.P. (1988): Introduction to Micrometeorology. London, Academic Press, 307 p.

ISHIKAKAWA, N., KOBAYASHI, S., OHATA, T. and KAWAGUCHI, S. (1982): Heat balance studies on sea ice near Syowa Station, East Antarctica. Mem. Natl Inst. Polar Res., Spec. Issue, **24**, 234–242.

MAKI, T. (1974): Turbulence characteristics and micrometeorological structure of atmospheric surface layer in stable stratification in Antarctica. Mem. Natl Inst. Polar Res., Ser. B (Meteorology), **2**, 65 p.

ONO, N. (1968): Kaihyô no netsu-teki seishitsu no kenkyû. IV. Kaihyô no netsu-teki na sho-teisû (Thermal properties of sea ice. IV. Thermal constants of sea ice). Teion Kagaku, Butsuri-Hen (Low Temp. Sci., Ser. A, Phys.), **26**, 329–349.

TAKEUCHI, K. and KONDO J. (1981): Chihyô ni Chikai Taiki (The Atmosphere Near the Ground). Tokyo, Tokyo Daigaku Shuppan Kai, 226 p.

WARREN, S.G. (1982): Optical properties of snow. Rev. Geophys. Space Phys., **20**, 67–89.

YAMANOUCHI, T., WADA, M., MAE, S., KAWAGUCHI, S. and TSUKAMURA, K. (1981): Measurements of radiation components at Mizuho Station, East Antarctica in 1979. Mem. Natl Inst. Polar Res., Spec. Issue, **19**, 27–39.

(*Received November 26, 1993; Revised manuscript received May 9, 1994*)